

Unconventional magnetostriction in layered $\text{La}_{1.2}\text{Sr}_{1.8}\text{Mn}_2\text{O}_7$: Evidence for spin-lattice coupling above T_C

D. N. Argyriou,* J. F. Mitchell, C. D. Potter, S. D. Bader, R. Kleb, and J. D. Jorgensen
*Science and Technology Center for Superconductivity and Materials Science Division, Argonne National Laboratory,
Argonne, Illinois 60439*

(Received 13 February 1997)

The crystal structure of $\text{La}_{1.2}\text{Sr}_{1.8}\text{Mn}_2\text{O}_7$ has been determined as a function of temperature in magnetic fields of 0 and 0.6 T. There is a significant magnetostriction at the Curie temperature T_C ; the a axis contracts ($\Delta a/a = -0.018\%$) while the c axis expands ($\Delta c/c = 0.05\%$). The latter value is larger than that found for perovskite manganites ($\Delta l/l = 0.02\%$ at 1 T). No such effect occurs at lower temperatures. The magnetostriction results from changes in individual Mn-O bond lengths. From T_C to ~ 300 K, bulk magnetization and magnetoresistance measurements indicate the presence of magnetic order not observed in the neutron-diffraction data. This suggests short-range magnetic order in this temperature range. Our structural measurements show that within this temperature interval there is also a weak magnetostriction. [S0163-1829(97)51018-6]

For a variety of hole-doped perovskite manganites, the application of a magnetic field results in an increase of the Curie temperature T_C and a decrease of the electrical resistance by orders of magnitude near T_C .¹ This colossal magnetoresistance (CMR) is broadly understood in terms of the double-exchange interaction between Mn^{3+} and Mn^{4+} ions.^{2,3} Here, e_g carriers can become itinerant but their conduction is spin dependent; the spin of the e_g carrier must be parallel to that of the localized Mn t_{2g} levels in order to maximize electrical conduction. Near T_C , application of an external magnetic field H can increase the parallel alignment of Mn spins and, thus, facilitate spin-polarized conduction of e_g carriers, to give rise to CMR. The double-exchange interaction also couples strongly to the crystal lattice through the Jahn-Teller effect on the Mn^{3+} ions, such that both charge-lattice^{4,5} and spin-lattice⁶ coupling have been observed in these materials.

The CMR is as high as 20 000% at 7 T (defined here as $100(\rho_H - \rho_0 T)/\rho_H\%$) for the layered Ruddlesden-Popper compound $\text{La}_{1.2}\text{Sr}_{1.8}\text{Mn}_2\text{O}_7$, as compared to $\sim 200\%$ at 7 T for similarly doped perovskite materials.⁷ Strong charge-lattice coupling has also been observed in layered $\text{La}_{1.2}\text{Sr}_{1.8}\text{Mn}_2\text{O}_7$;⁸ at the metal-insulator transition (MI) the a axis contracts due to the contraction of the planar Mn-O bonds while the c axis sharply expands. In this paper we report the direct investigation of the spin-lattice coupling in layered $\text{La}_{1.2}\text{Sr}_{1.8}\text{Mn}_2\text{O}_7$ by determining its structure in 0 and 0.6 T as a function of temperature. Despite the relatively small applied field, we find that the magnetostriction is significant at 0.6 T; a small contraction of the a axis ($\sim -0.018\%$) and a larger expansion of the c axis ($\sim 0.05\%$) relative to zero field is observed at T_C . The latter value is larger than that for perovskite manganites.⁴ We demonstrate that these changes arise directly from field-induced changes of individual Mn-O bond lengths. Our results also indicate that there is a weak spin-lattice coupling above T_C that persists close to room temperature. This observation suggests the existence of short-range magnetic ordering in

this extended temperature interval. The observed magnetic properties over the same temperature interval support such a conclusion.

Crystals of $\text{La}_{1.2}\text{Sr}_{1.8}\text{Mn}_2\text{O}_7$ were melt grown in flowing 20% O_2 (balance Ar) in a floating-zone, optical-image furnace (NEC SC-M15HD). As seen from Fig. 1, the sample exhibits an MI transition at 120 K, in good agreement with the report of Moritomo *et al.*⁷ Figure 1(a) shows the CMR; in 1 T it is 280% and it increases to 5800% at 5 T. We also note that the MI transition temperature increases with H ; it is 120 K for 0 T and 156 K in 5 T. The MI transition is coupled to a ferromagnetic transition at $T_C = 120$ K, as seen in Fig. 4(a) (these data will be discussed further below). The bulk magnetization measurements, Fig. 1(b), illustrate the evolution of magnetism in this sample from a paramagnetic state at 350 K to a ferromagnetic state below T_C . An intermediate state is observed at 150 and 130 K.

Time-of-flight neutron powder-diffraction data were collected as a function of temperature in $H = 0$ and 0.6 T on the Special Environment Powder Diffractometer (SEPD)⁹ at Argonne's Intense Pulsed Neutron Source (IPNS). For the in-field measurement Nd-Fe-B permanent magnets of dimensions $5.4 \times 2.5 \times 1$ cm were used. The magnets were placed behind stainless steel poles and screened from the beam with cadmium. The gap between the poles was 8 mm. The sample, contained in a vanadium can, was placed between the poles. A field of 0.6 T with a homogeneity of 3% over the length of the poles, was measured in the sample position using a Hall probe. For the measurement of diffraction data, the magnetic assembly was attached to a Displex, and data were collected as a function of temperature. Neutron powder-diffraction patterns of $\text{La}_{1.2}\text{Sr}_{1.8}\text{Mn}_2\text{O}_7$ are consistent with a tetragonal cell, space group $I4/mmm$, at all temperatures and H values explored. Powder-diffraction patterns were analyzed with the Rietveld method using the program GSAS.¹⁰ The crystal structure of $\text{La}_{1.2}\text{Sr}_{1.8}\text{Mn}_2\text{O}_7$ consists of double perovskite layers, each layer made up of a two-dimensional (2D) layer of MnO_6 octahedra. The (La,Sr) at-

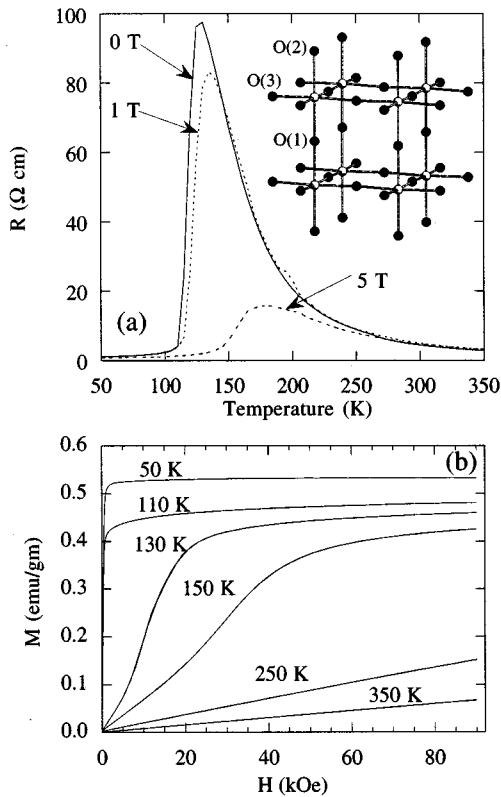


FIG. 1. (a) Resistivity in 0, 1, and 5 T fields and (b) magnetization loops measured at various temperatures. The double perovskite layer of the $\text{La}_{1.2}\text{Sr}_{1.8}\text{Mn}_2\text{O}_7$ is shown in the inset of the upper panel; the labeling of the O atoms used in this paper is shown. Mn atoms are not labeled and (La,Sr) atoms are not shown.

oms separate the double layers. A portion of the crystal structure of $\text{La}_{1.2}\text{Sr}_{1.8}\text{Mn}_2\text{O}_7$ can be seen in the inset of Fig. 1(a).

The effect of H on the temperature dependence of the lattice parameters of $\text{La}_{1.2}\text{Sr}_{1.8}\text{Mn}_2\text{O}_7$ is illustrated in Fig. 2. Remarkably, this effect is significant even in a small magnetic field. We first note that the lattice effect associated with the MI and Curie transition increases in temperature by ~ 4 K for 0.6 T, in agreement with the effect of H on the MI transition temperature [Fig. 1(a)]. Secondly, both the c and a axis show appreciable magnetostriction. This is most noticeable for the c axis; with decreasing temperature the c axis decreases to $20.0553(3)$ Å at $T_C = 124$ K, a value higher by $0.0070(4)$ Å than that observed at $T_C = 120$ K for the 0 T measurement. The magnetostriction for the c axis is maximal at 115 K, $\Delta c/c$ is $\sim 0.05\%$ (see upper inset in Fig. 2). The a axis shows a smaller and opposite magnetostriction compared to the c axis; with decreasing temperature the a axis saturates to a slightly lower value in 0.6 T compared to zero field. Again the a axis magnetostriction is maximal at 115 K, $\Delta a/a \sim 0.018\%$ (see lower inset in Fig. 2). Ibarra *et al.*⁴ have measured the linear thermal expansion of the perovskite $\text{La}_{0.6}\text{Y}_{0.07}\text{Ca}_{0.33}\text{MnO}_3$ in different fields (up to 12 T). From their data it is evident that the difference in $\Delta l/l$ between 0 and 1 T is $\sim 0.02\%$. This value is comparable to ours for the a axis, but smaller than ours for the c axis (despite our smaller field). This suggests that within the MnO_2 planes the

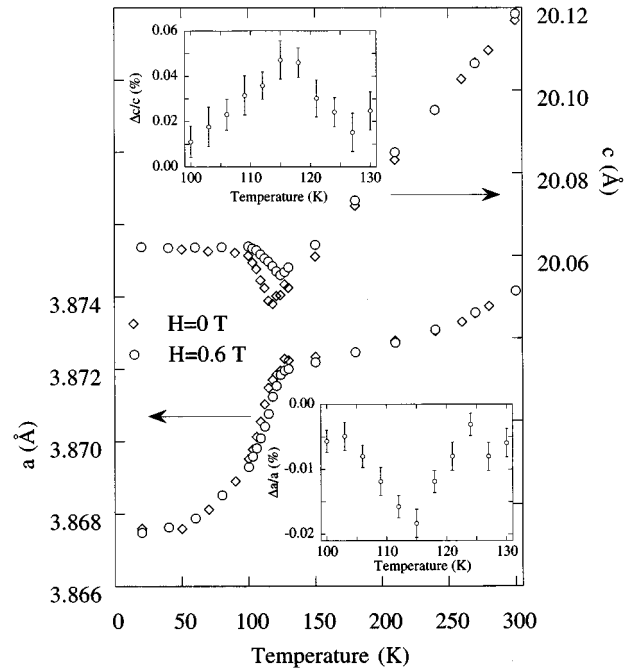


FIG. 2. a and c lattice parameters as functions of temperature in 0 and 0.6 T. Values of $\Delta c/c$ and $\Delta a/a$ are shown in the insets. The errors in a and c are smaller than the plot symbols.

double exchange interaction is similar in strength to that in perovskite materials. The significantly larger response perpendicular to the MnO_2 planes in the layered compound suggests a different mechanism for the magnetostrictive response of the c axis. Below T_C the magnetostriction converges to zero, as is the case for the 3D perovskite manganites.

We find that the magnetostriction results directly from changes in individual Mn-O bond lengths. The relevant bonds are the four planar Mn-O(3) bonds and the apical Mn-O(2) bond (see inset of Fig. 1), while the Mn-O(1) bond length and the Mn-O(3)-Mn bond angle remain unchanged within experimental error in different H . The response of the Mn-O(2) bond is significant, as can be seen in Fig. 3; the Mn-O(2) bond closely mimics the c axis in that just above T_C it reaches a higher value in 0.6 T than in 0 T. Note that Mn-O(2) increases by $\sim 1\%$ upon cooling through the MI transition when $H=0$ T, but by less than half this amount in 0.6 T. This further demonstrates that even a small field can have dramatic influence on the lattice anomalies associated with the delocalization of charge in this layered material. Also, as with the a axis, the contraction of the Mn-O(3) in applied field is small and localized to a small temperature window surrounding T_C .

The cooperative contraction of the Mn-O(3) bond and expansion of the Mn-O(2) bond at the onset of charge delocalization⁸ and the application of a magnetic field, suggest a compensation mechanism for the distortion of the MnO_6 octahedron through these transitions. The conserved quantity appears to be the valence at the Mn site. This can be estimated by the bond valence sum method,¹¹ where the valence at the Mn site is given by

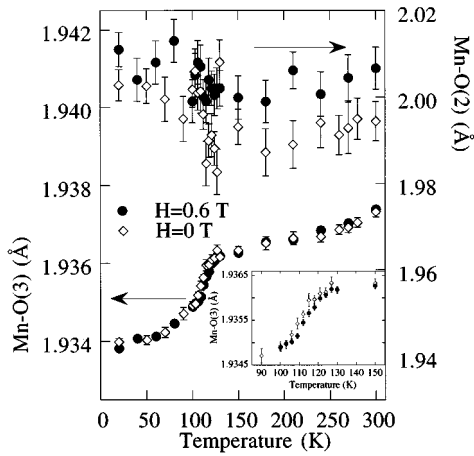


FIG. 3. Variation of the Mn-O(2) and Mn-O(3) bond lengths as a function of temperature in 0 and 0.6 T.

$$V_{\text{Mn}} = \sum_i \exp[(r_0 - r_i)/B],$$

and where $r_0 = 1.757 \text{ \AA}$, $B = 0.37 \text{ \AA}$, and the sum is over the six measured Mn-O bond lengths, r_i . Calculation of the bond-valence sum shows that V_{Mn} changes little across the MI and ferromagnetic transitions, despite the dramatic changes in the Mn-O bonds; in 0 T the bond valence sum, V_{Mn} , varies from 3.610 to 3.615 across T_C , while in 0.6 T, V_{Mn} varies from 3.597 to 3.601. The cooperative behavior of the Mn-O bonds stems from the structure of $\text{La}_{1.2}\text{Sr}_{1.8}\text{Mn}_2\text{O}_7$ which allows the MnO_6 octahedra an extra degree of freedom not found in the 3D perovskites. In the a - b plane, the O(3) oxygen atoms are part of infinite 2D Mn-O-Mn linkages. In contrast, the O(2) atom is part of a shorter O(2)-Mn-O(1)-Mn-O(2) linkage and is covalently bonded to only one Mn atom while ionically bonded to five (La,Sr) atoms. This configuration allows the Mn-O(2) bond to respond to changes in the Mn-O(3) bonds to maintain a nominally constant average bond length characteristic of the nominal Mn valence. This conservation of Mn valence is somewhat unexpected in light of the charge delocalization associated with the MI transition.

The magnetostriction effects described here cannot result simply from an increase of T_C due to an applied field; that would simply increase the temperature at which the lattice effect occurs, without altering its magnitude. To the contrary, our observations suggest that the effect is a result of strong spin-lattice coupling in this layered compound. Application of the magnetic field increases the alignment of Mn spins in the a - b plane,⁸ and thus enhances the spin-polarized conductivity of e_g electrons in MnO_2 sheets close to T_C ; this enhancement in conductivity in turn results in a further contraction of the planar Mn-O(3) bonds in response to localized charge moving out of Mn-O antibonding orbitals to become carriers. The surprising observation is that application of a small field results in a large magnetostriction in $\text{La}_{1.2}\text{Sr}_{1.8}\text{Mn}_2\text{O}_7$, larger than that found in the 3D perovskites, as illustrated by the behavior of the c axis. Such a magnetostriction can be understood as a response to the small contraction of the Mn-O(3) bond in field. At the MI

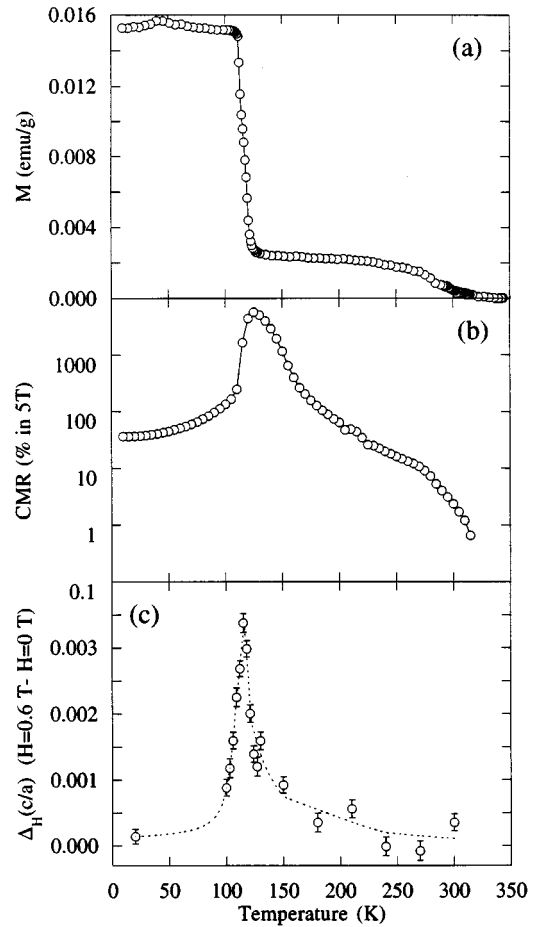


FIG. 4. (a) Magnetization in a field of 30 G, (b) CMR, defined as $(\rho_{0T} - \rho_{5T})/\rho_{5T}(\%)$ and (c) $\Delta_H(c/a)$, as a function of temperature. The line is a guide to the eye.

transition, the contraction of the Mn-O(3) bond is compensated by the expansion of the Mn-O(2) bond to maintain a mean equilibrium Mn-O bond length consistent with a constant nominal Mn valence. Similarly, the additional in-field contraction of the Mn-O(3) bond is further compensated by an expansion of the Mn-O(2) bond. Thus, the Mn-O(2) bond and the c axis are extremely sensitive parameters not only to changes in the electronic properties, but also to the magnetic properties of this layered compound.

Above T_C we observe that the low-field magnetization is nonzero [Fig. 4(a)], and decreases to zero gradually at approximately 300 K. Resistivity measurements indicate some magnetoresistance in this region as seen in Fig. 4(b), while magnetization data shown in Fig. 1(b) indicate an intermediate magnetic state between the paramagnetic-type behavior, observed at 350 K and the ferromagnetic state below T_C . This temperature region T_C to 300 K has been identified with the presence of a magnetic short-range ordering of Mn spins.^{8,11} Interestingly, our structural data suggest that there is a weak coupling between the lattice and this short-ranged magnetic state. Figure 4(c) shows $\Delta_H(c/a)(c/a(H=0.6 \text{ T}) - c/a(H=0 \text{ T}))$ as a function of temperature; with increasing temperature $\Delta_H(c/a)$ rapidly increases to its maximum value at 115 K [$\Delta_H(c/a) = 0.0034(2)$], but decreases slowly to zero above

T_C [$\Delta_H(c/a)=0.0009(1)$ at 150 K, $0.0006(1)$ at 210 K] indicating a weak magnetostriction between T_C and ~ 300 K.

In this paper we show that the application of a small magnetic field leads to a substantial magnetostriction in layered $\text{La}_{1.2}\text{Sr}_{1.8}\text{Mn}_2\text{O}_7$. At T_C and in 0.6 T the a axis contracts by $\sim -0.018\%$ and the c axis expands by $\sim 0.05\%$. The latter change is larger than that reported for the perovskite manganites. We suggest that the contraction of the Mn-O(3) bond is a response to the increased spin-polarized conductivity of e_g carriers in 0.6 T, while the larger expansion of the Mn-O(2) bond is a response to maintain a constant Mn valence.

Our structural probe indicates that above T_C to ~ 300 K a weak magnetostriction effect associated with a short-range ordered state as revealed by magnetization and MR results is found.

This work was supported by the U.S. Department of Energy, Basic Energy Sciences-Materials Sciences, and ER-LTR, under Contract No. W-31-109-ENG-38 (J.F.M., C.D.P., R.K., S.D.B., J.D.J.) and by the NSF Office of Science and Technology Centers under Grant No. DMR-91-20000 (DNA).

*Present address: Los Alamos Neutron Science Center, MS H805, Los Alamos National Laboratory, Los Alamos, New Mexico 87545.

¹H. Y. Hwang, S.-W. Cheong, P. G. Radaelli, M. Marezio, and B. Batlog, *Phys. Rev. Lett.* **75**, 914 (1995).

²C. Zener, *Phys. Rev.* **51**, 403 (1951).

³P. D. deGennes, *Phys. Rev.* **118**, 141 (1960).

⁴M. R. Ibarra, P. A. Algarabel, C. Marquina, J. Blasco, and J. Garcia, *Phys. Rev. Lett.* **75**, 3541 (1995).

⁵P. G. Radaelli, D. E. Cox, M. Marezio, S.-W. Cheong, P. E. Schiffer, and A. P. Ramirez, *Phys. Rev. Lett.* **75**, 4488 (1995).

⁶D. N. Argyriou, J. F. Mitchell, C. D. Potter, D. G. Hinks, J. D.

Jorgensen, and S. D. Bader, *Phys. Rev. Lett.* **76**, 3826 (1996).

⁷Y. Moritomo, A. Asamitsu, H. Kuwahara, and Y. Tokura, *Nature (London)* **380**, 141 (1996).

⁸J. F. Mitchell, D. N. Argyriou, J. D. Jorgensen, D. G. Hinks, C. D. Potter, and S. D. Bader, *Phys. Rev. B* **55**, 63 (1997).

⁹J. D. Jorgensen, J. J. Faber, J. M. Carpenter, R. K. Crawford, J. R. Haumann, R. L. Hitterman, R. Kleb, G. E. Ostrowski, F. J. Rotella, and T. G. Worton, *J. Appl. Crystallogr.* **22**, 321 (1989).

¹⁰A. C. Larson and R. B. von Dreele, *General Structure Analysis System*, University of California (1985–1990).

¹¹T. Kimura, Y. Tomioka, H. Kuwahara, A. Asamitsu, M. Tamura, and Y. Tokura, *Science* **274**, 1698 (1996).